BIOCHEMISTRY
including biophysical chemistry & molecular biology

Article

pubs.acs.org/biochemistry

Thermodynamic Analysis of Transition-State Features in Picomolar Inhibitors of Human 5′-Methylthioadenosine Phosphorylase

Rong Guan,[†] Peter C. Tyler,[‡] Gary B. Evans,[‡] and Vern L. Schramm*[,†]

[†]From the Department of Biochemistry, Albert Einstein College of Medicine, Yeshiva University, 1300 Morris Park Avenue, Bronx, New York 10461, United States

[‡]Carbohydrate Chemistry, Callaghan Innovation, Ltd., PO Box 31-310, Lower Hutt 5040, New Zealand

ABSTRACT: Human 5′-methylthioadenosine phosphorylase (MTAP) is solely responsible for 5′-methylthioadenosine (MTA) metabolism to permit S-adenosylmethionine salvage. Transition-state (TS) analogues of MTAP are in development as anticancer candidates. TS analogues of MTAP incorporate a cationic nitrogen and a protonated 9-deazaadenine leaving group, which are mimics of the ribocation transition state. MT-ImmA and MT-DADMe-ImmA are two examples of these TS analogues. Thermodynamic analysis of MTA, inhibitor, and phosphate binding reveals the cationic nitrogen to provide −2.6 and −3.6 kcal/mol binding free energy for MT-ImmA and MT-DADMe-ImmA, respectively. The protonated deazaadenine provides an additional −1.3 (MT-ImmA) to −1.7 kcal/mol (MT-DADMe-ImmA). MT-DADMe-ImmA is a better match in TS geometry than MT-ImmA and is thermodynamically favored. Binding of TS analogues to the MTAP/phosphate complex is fully entropic, in contrast to TS analogue binding to the related human purine nucleoside phosphorylase/phosphate complex, which is fully enthalpic (Guan, R., Ho, M. C., Brenowitz, M., Tyler, P. C., Evans, G. B., Almo, S. C., and Schramm, V. L. (2011) *Biochemistry* *50*, 10408−10417). The binding thermodynamics of phosphate or TS analogues alone to MTAP are fully dominated by enthalpy. Phosphate anchored in the catalytic site forms an ion pair with the cationic TS analogue to cause stabilization of the enzyme structure in the ternary complex. The ternary-induced conformational changes convert the individual enthalpic binding energies to entropy, resulting in a presumed shift of the protein architecture toward the transition state. Formation of the ternary TS analogue complex with MTAP induces a remarkable increase in thermal stability (ΔT_m 28 °C). The enthalpic, entropic, and protein-stability features of TS analogue binding to human MTAP are resolved in these studies.

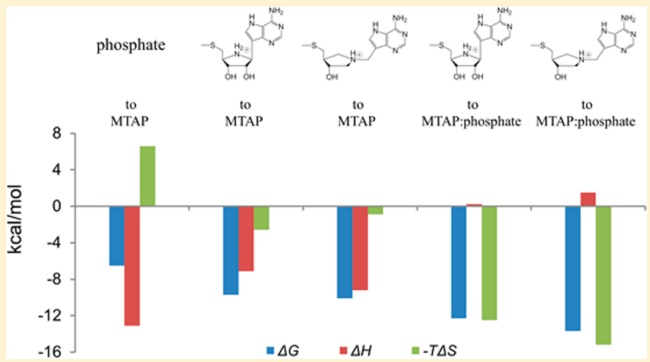

The metabolite 5′-methylthioadenosine (MTA) links the polyamine biosynthesis and S-adenosyl-L-methionine (SAM) recycling pathways. MTA in humans is produced exclusively from decarboxy-SAM during the biosynthesis of spermine and spermidine.[1] MTA is metabolized only through the phosphorolysis catalyzed by 5′-methylthioadenosine phosphorylase (MTAP) to adenine and 5-methylthioribose-1-phosphate. Adenine is recycled to the adenylate pool via adenine phosphoribosyltransferase, and 5-methylthioribose-1-phosphate is recycled to methionine (precursors of SAM recycling).[2,3] There is no significant MTA in normal mammalian tissues, but inhibition of MTAP in mice causes accumulation of MTA in blood and urine, and in rare human deficiencies of MTAP, MTA is also found in the blood.[4−6] Although the metabolic effects of MTA accumulation are incompletely understood, feedback inhibition of polyamine biosynthesis and inhibition of SAM salvage from MTA have been proposed.[4] Altered SAM pools are then proposed to influence epigenetic control via protein and DNA methylations and thus inhibit the proliferation of cancer cells.[4] The unique role of human MTAP in MTA metabolism supports its significance as an anticancer target.[4,5]

Transition-state (TS) analysis for MTAP used kinetic isotope effects and quantum computational chemistry to aid in the design of TS analogue inhibitors.[7] A late dissociative TS was proposed to include a cationic ribosyl anomeric carbon and an anionic leaving group (Figure 1A).[7] On the basis of this TS structure, two generations of TS analogue inhibitors were synthesized but with N7 protonated to mimic the anionic N7 stabilized by hydrogen bonding with a proton of Asp220 at the TS. Analogues with similarity to the TS exhibited high binding affinity to the MTAP/phosphate complex.[8−10] MT-ImmA and MT-DADMe-ImmA are examples of first- and second-generation TS analogues for MTAP, with dissociation constants of 1 nM and 90 pM, respectively. Substitutions for the 5′-methylthio group can increase the affinity; thus, the K_d for pClPhT-DADMe-ImmA is 10 pM (Figure 1B).[9,10] These inhibitors possess TS features with a cationic nitrogen mimicking the cationic anomeric carbon and the 9-

Received: August 28, 2013
Revised: October 4, 2013
Published: October 22, 2013

   dx.doi.org/10.1021/bi401188w | *Biochemistry* 2013, 52, 8313−8322

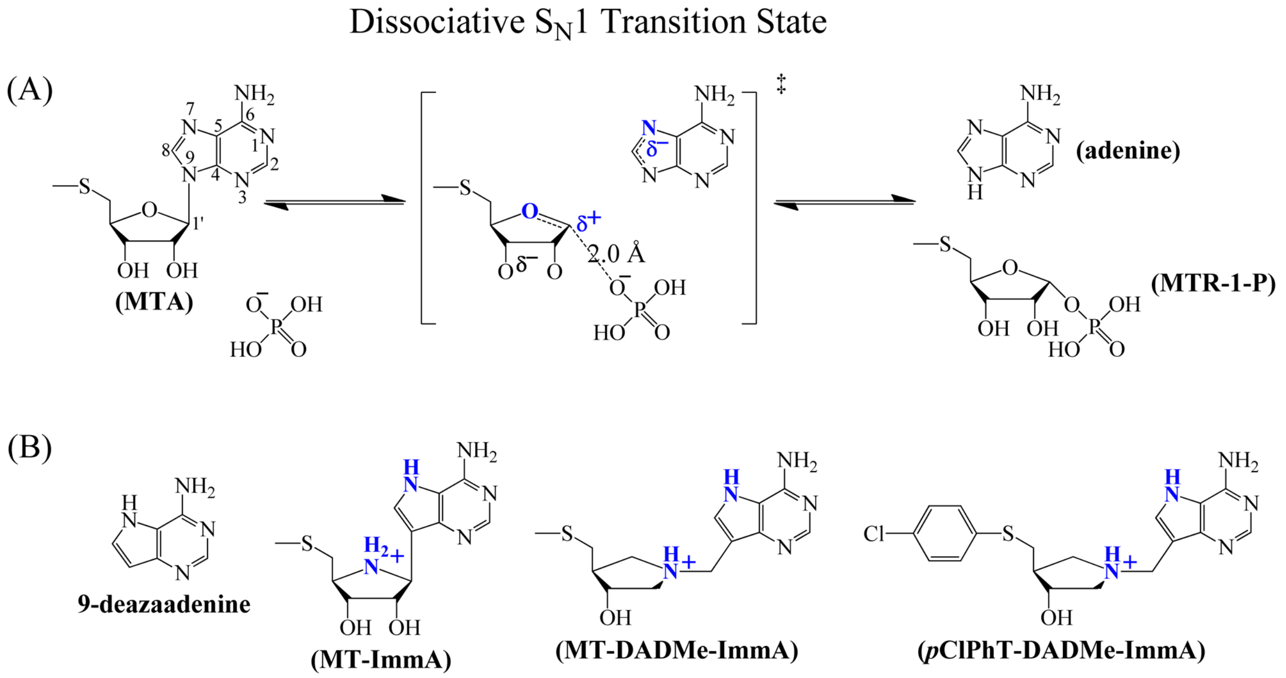

Figure 1. (A) Transition state of MTAP. (B) Transition-state analogue inhibitors of MTAP. The 9-deazaadenine group increases the pK_a of N7 (blue). MT-ImmA and MT-DADMe-ImmA are first and second generations of transition-state analogues, respectively. pClPhT-DADMe-ImmA is a 10 pM inhibitor of MTAP. Transition-state features and their mimics in transition-state analogues are in blue.

deazaadenine mimicking the adenine leaving group. MT-ImmA has only a single C−N bond distance (1.5 Å) between the cationic nitrogen and the leaving group, resembling a substrate-like early TS. MT-DADMe-ImmA increases that distance to 2.8 Å, through incorporation of a methylene bridge, to reflect more accurately the geometry of the late dissociative TS and hence shows the tighter binding affinity. In immunodeficient mice, treatment with MT-DADMe-ImmA causes remission of human head and neck cancer and suppresses the growth and metastases of human lung cancer.[4,5] The high efficacy and low toxicity of MT-DADMe-ImmA suggests potential as a new approach for cancer treatment.

Isothermal titration calorimetry (ITC) studies were used earlier to explore the tight binding of TS analogues to the MTAP/phosphate complex.[11] The analysis revealed an unexpected thermodynamic signature with favorable entropy but unfavorable enthaply upon formation of the ternary TS analogue complex. MTAP and its homologous enzyme, human purine nucleoside phosphorylase (HsPNP), share similar overall structures and related TS analogue inhibitors.[12,13] Both enzymes are homotrimers with three active sites located near the subunit interfaces. The enzymes differ in catalytic site cooperativity. Filling a single catalytic site of HsPNP fully inhibits the enzyme, whereas all three sites of MTAP must be filled with TS analogues to cause complete inhibition.[11,14] Binding of TS analogues to the HsPNP/phosphate complex is driven by a favorable enthalpy with entropic penalties, opposite to the thermodynamic signature for MTAP.[11,13] The entropically driven binding of TS analogues to MTAP was surprising because the crystal structures of HsPNP and MTAP with TS analogues show similar hydrogen-bond and ionic-bond interactions but opposite thermodynamic patterns. The pattern with MTAP suggested an increased order in the enzyme active site and the overall protein structure, causing the release of water from the subunit interfaces and especially from the active site.[11] The most significant conformational change was observed for a loop of nine amino acid residues, 227−235, which is flexible in the apo enzyme but is ordered in the ternary TS analogue complexes.[11] The ordered loop blocks the solvent channel to the enzyme active site and expels the water inside, consistent with the observed entropic binding. The distinct thermodynamic signatures of MTAP and HsPNP for binding to their TS analogues suggest that even closely related enzymes have specifically evolved mechanisms of converting substrates to the TS.[11]

Previous thermodynamic studies of MTAP focused on the formation of the ternary TS analogue complex.[11] Here, we dissect the binding of individual phosphate and TS analogue components to the apo enzyme and subsequent formation of the ternary complex. The binding thermodynamics of each component is explored to provide full thermodynamic cycles for TS analogue binding. Contributions to binding free energy are derived from thermodynamic cycles for both generations of TS analogues. Thermodynamic signatures are also determined for each component with evaluation and corrections for the protonation effects on binding and are evaluated in terms of the entropic driving force for the formation of complexes proposed to be related to the functional TS complex. Finally, we experimentally verify that the ternary complex with bound TS analogue is highly stabilized to heat denaturation. Thus, the entropically driven formation of the ternary complex reflects solvent reorganization and not protein destabilization toward a denatured state. This work provides insights into the thermodynamic nature of TS analogue interactions with MTAP. The unique mechanisms of converting binding enthalpy to entropy provide a general lesson on TS analogue interactions with their targets.

Table 1. Thermodynamic Parameters for Ligands Binding to Apo MTAP in Hepes Buffer

ligand	K_d (nM), [n][a]	ΔG (kcal/mol)	ΔH_{Hepes} (kcal/mol)	$-T\Delta S_{Hepes}$ (kcal/mol)
MT-ImmA	70 ± 10 [3]	−9.7 ± 0.1	−9.59 ± 0.08	−0.1 ± 0.1
MT-DADMe-ImmA	40 ± 10 [2]	−10.1 ± 0.2	−10.2 ± 0.8	0.1 ± 0.8
	110 ± 20 [1]	−9.5 ± 0.1	−3 ± 1	−7 ± 1
phosphate	17 000 ± 2000 [3]	−6.51 ± 0.06	−8.7 ± 0.3	2.2 ± 0.3
MTA	8 ± 5 [1]	−11.1 ± 0.4	−1.0 ± 0.3	−10.1 ± 0.5
	700 ± 100 [2]	−8.4 ± 0.1	−6.1 ± 0.2	−2.3 ± 0.2

[a] n is the number of sites.

MATERIALS AND METHODS

Chemicals. MT-ImmA and MT-DADMe-ImmA were synthesized as described elsewhere.[9,10] MTA and potassium phosphate were purchased from Sigma. All other chemicals and reagents were obtained from either Sigma or Fisher Scientific and were of the highest grades of purity available.

Enzyme Preparation. The purification of human MTAP has been detailed previously.[12] Briefly, a plasmid containing the synthetic gene of *MTAP* was transformed into BL21-CodonPlus(DE3)-RIPL *Escherichia coli* cells. Cells were grown at 37 °C in LB medium containing 100 μg/mL of ampicillin, and expression was induced by addition of 1 mM IPTG (final concentration). Cells were collected and disrupted by a french press. The supernatant was loaded onto a Ni-NTA superflow column for purification. MTAP was eluted with a buffer containing 50 mM phosphate, 300 mM NaCl, and 80 mM imidazole at pH 8.0. Purified enzyme was dialyzed against 100 mM phosphate, pH 7.4, with 5 mM DTT and stored at −80 °C. Recombinant MTAP contains 14 additional amino acids at the N-terminus, including a His_6 tag, and is catalytically equivalent to the native enzyme. The additional N-terminal residues are far away from the active site and are disordered in the crystal structures.[12] The expressed form of human MTAP has an estimated extinction coefficient of 30.94 mM^{-1} cm^{-1} at 280 nm, which is the constant used to estimate protein concentrations (ProtParam program from ExPASy).

Isothermal Titration Calorimetry Studies. Purified MTAP exists as homotrimer and, as purified above, approximately two-third of the active sites are occupied by its product, adenine. Copurified adenine was removed by dialyzing the enzyme against 0.5% (V/V) charcoal in 100 mM phosphate, pH 7.4, for 3 h.[12] Adenine-free MTAP was further dialyzed against a buffer containing 50 mM Hepes and 100 mM NaCl at pH 7.4 with at least three buffer changes to obtain apo enzyme free of bound phosphate. ITC studies were performed on a VP-ITC MicroCalorimeter. Dialysate and apo MTAP were filtered (Millipore, 0.2 μm) right before experiments. The filtered dialysate was used as solvent to prepare the ligand solutions. MTAP sample (40 μM) and ligand solution (600 μM) were degassed (Microcal Thermovac) for 15 min and loaded into a 1.46 mL sample cell and 250 μL injection syringe of the calorimeter, respectively. Isothermal titrations included 20−30 injections of 4−6 μL of inhibitor solutions, with a spacing of 230 s between injections. Human MTAP slowly hydrolyzed MTA in the absence of phosphate with a k_{cat} of (5.1 ± 0.1) × 10^{-5} s^{-1} as estimated by UPLC. To avoid significant hydrolysis of MTA, ITC experiments for MTA used a low concentration of enzyme (25 μM) and MTA (350 μM), with 18 injections at 9 μL/injection, and a shorter interval time of 180 s. To explore the protonation/deprotonation effect on the binding of inhibitors and phosphate, ITC studies were carried out in a buffer (50 mM Tris and 100 mM NaCl at pH 7.4) with a different ionization enthalpy from the HEPES buffer. Other experimental conditions were kept the same as described above. Isothermal titrations were performed at 25 °C and were initiated with adenine-free and phosphate-free apo enzyme. Heat of dilution corrections were added from control experiments by titrating the ligand into buffer.

ITC Data Processing. ITC data of MT-ImmA (first-generation inhibitor) and phosphate titrations gave the best results when fitted to the single set of identical sites model. Data of MT-DADMe-ImmA (second-generation inhibitor) and MTA binding fit the best to a model for two sets of independent sites. Dissociation constants (K_d) for those ligands were determined from the ITC-data fitting. ΔG values were calculated from K_d using eq 1. The entropy terms ($-T\Delta S$) were calculated from eq 2 (the Gibbs free-energy expression).

$$\Delta G = RT\ln K_d \tag{1}$$

$$\Delta G = \Delta H - T\Delta S \tag{2}$$

Equations 3 and 4 represent the total heat content of the solution (Q) contained in the active cell volume (V_0) for a single set of identical sites and two sets of independent sites, respectively. Equation 5 represents the heat released (ΔQ_i) from the ith injection in an ITC experiment. In eqs 3−5, n is the number of sites, Θ is the fraction of sites occupied by ligand, dV_i is the injection volume, M_t is the concentration of the protein in V_0, and ΔH is the molar heat from inhibitor binding. ITC data were fitted using software Origin 7.0 and followed the same procedures for single set of identical sites and two sets of independent sites models. Initial guesses of n, K_a, and ΔH were generated by the algorithm. (K_a is the association constant of ligand, the reciprocal of dissociation constant K_d. K_i is the dissociation constant of inhibitors.) ΔQ_i for each injection was calculated and compared with the corresponding heat obtained from experiment. The values of n, K_a, and ΔH were optimized using standard Marquardt methods and iterated to reach the best fit to the model. The n value has been determined to be 3 for human MTAP and was directly input into Origin 7.0 for accurate fitting.[12] More details of the data processing are available in the user's manual for the VP-ITC MicroCalorimeter.

$$Q = n\Theta M_t \Delta H V_0 \tag{3}$$

$$Q = M_t V_0 (n_1 \Theta_1 \Delta H_1 + n_2 \Theta_2 \Delta H_2) \tag{4}$$

$$\Delta Q_i = Q_i + \frac{dV_i}{V_0}\left(\frac{Q_i + Q_{i-1}}{2}\right) - Q_{i-1} \tag{5}$$

Differential Scanning Fluorimetry Studies. A 7900HT fast real-time PCR system was used to conduct the differential temperature scanning fluorimetry experiments of MTAP. Samples of 10 μL were monitored in wells of a 384-well

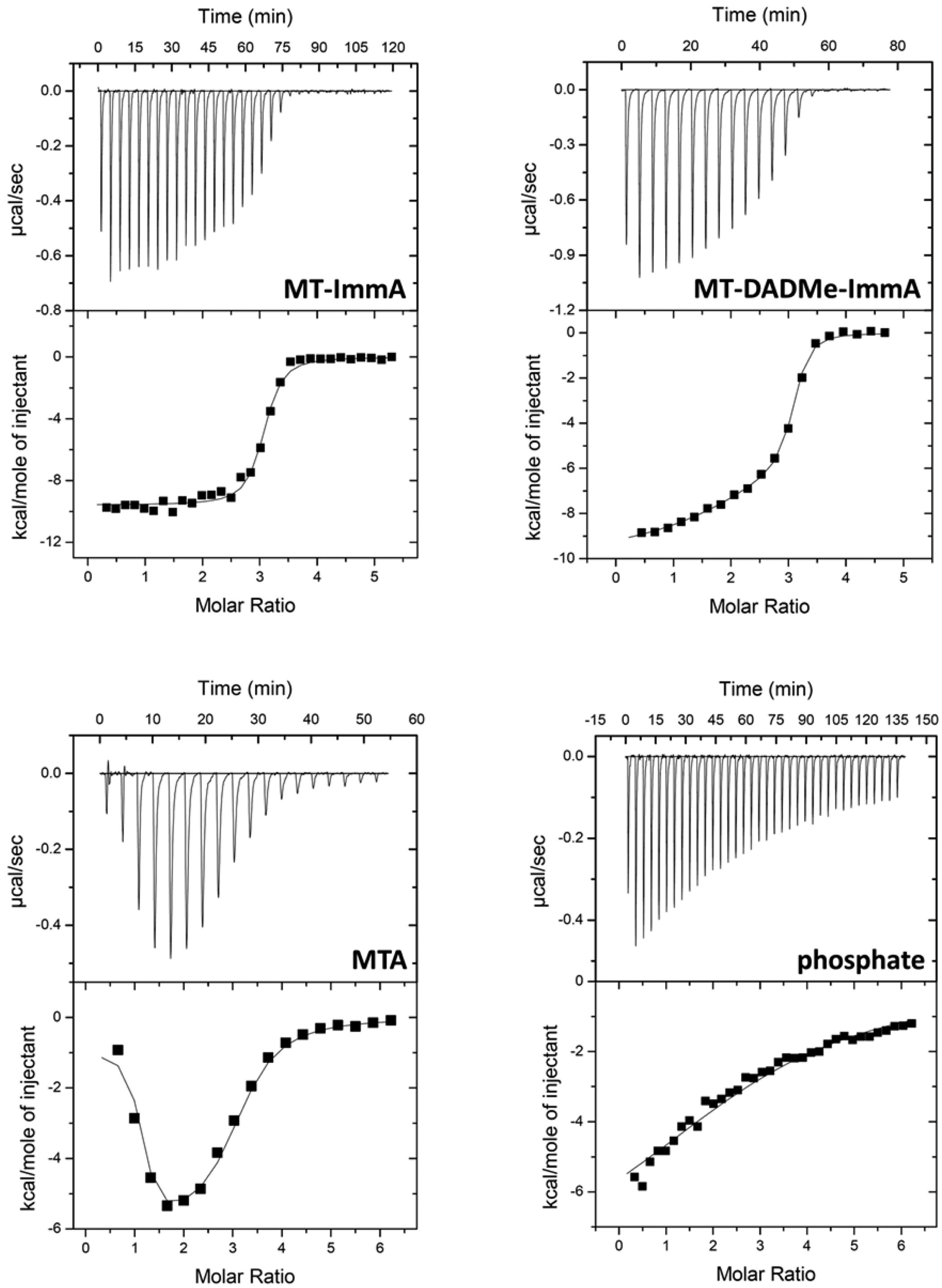

Figure 2. Isothermal titrations of apo MTAP with ligands in Hepes Buffer.

plate, with 10 replicates for each condition, containing 50 mM Hepes (pH 7.4), 100 mM NaCl, 25 μM MTAP, 1× Sypro Orange (from vendor solution), 0 or 20 mM phosphate, and 0 or 500 μM TS analogues. A control was included without enzyme, phosphate, or TS analgoues. The melting temperatures (T_m values) were determined as described earlier using GraFit 5 (Erithacus Software) and the Boltzmann equation.[16]

■ RESULTS AND DISCUSSION

MT-ImmA and MT-DADMe-ImmA possess a cationic nitrogen and protonated N7 to mimic two main TS features of MTAP (Figure 1). MT-ImmA represents the substrate-like early TS with a 1.5 Å single C−N bond between the cationic ribosyl mimic and the leaving group. MT-DADMe-ImmA extends the distance to 2.8 Å with a methylene group insertion, a mimic of a late TS geometry. Thermodynamics of TS analogue inhibitor binding to the MTAP/phosphate complex is entropically driven, but thermodynamics of the binding of phosphate and TS analogue to the apo MTAP is needed to understand the binding order, cooperativity of binding, and the thermodynamic cycle. ITC studies were carried out for binding of MT-ImmA, MT-DADMe-ImmA, phosphate, and MTA to apo MTAP in

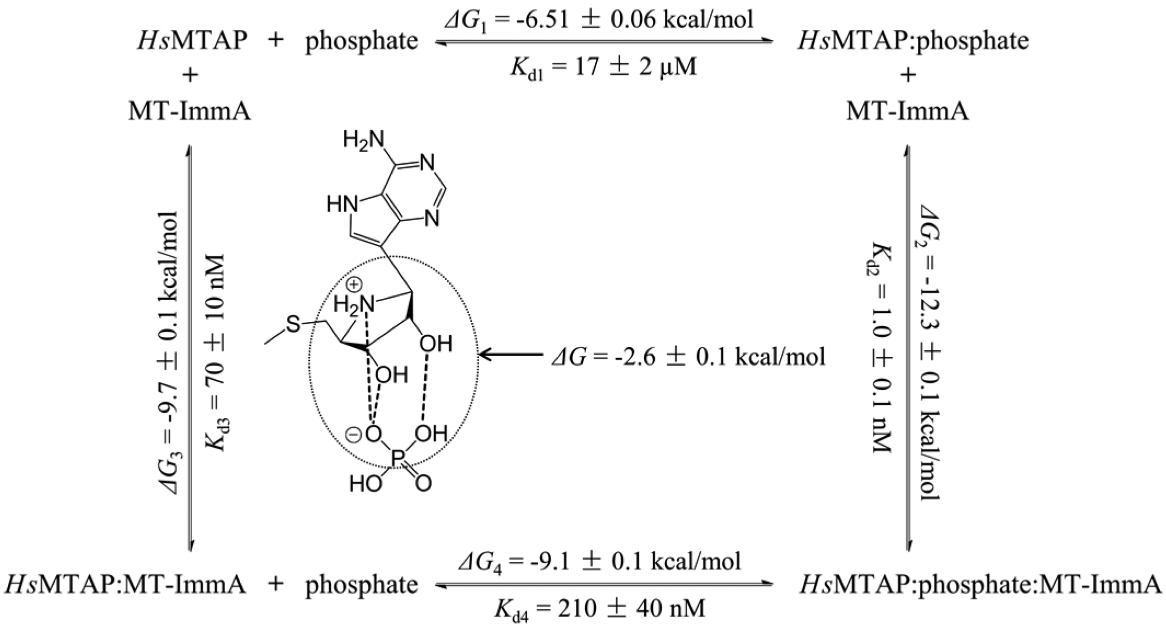

Figure 3. Thermodynamic cycle of MT-ImmA and phosphate binding to MTAP. MT-ImmA is a first-generation transition-state analogue inhibitor of MTAP. The ΔG and K_d values of MT-ImmA binding to MTAP/phosphate complex are from ref 11. The interaction between MT-ImmA and phosphate is indicated as dashed lines.

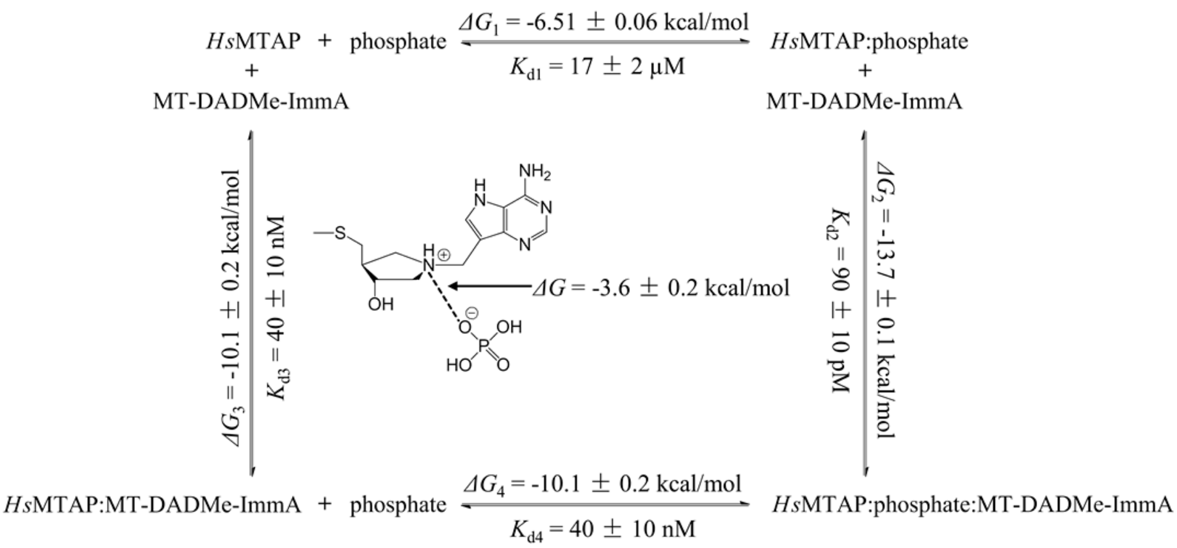

Figure 4. Thermodynamic cycle of MT-DADMe-ImmA and phosphate binding to MTAP. MT-DADMe-ImmA represents second-generation transition-state analogue inhibitors of MTAP. The ΔG and K_d values of MT-DADMe-ImmA binding to MTAP/phosphate complex are from ref 11. The interactions between MT-DADMe-ImmA and phosphate are indicated as dashed lines.

Hepes buffer to resolve the complete thermodynamic cycles for the binding of both generations of inhibitors. Analysis of the thermodynamic cycles provides estimates of the thermodynamic contributions from the cationic nitrogen upon inhibitor binding. The comparison of binding free energy for MTA relative to the TS analogues also provides an estimation of thermodynamic contributions from the 9-deazaadenine group.

Affinity and Binding Free Energy of Ligands to Apo MTAP. The dissociation constants and binding free energy of ligands to apo MTAP were obtained from ITC experiments in Hepes buffer (Table 1 and Figure 2). MT-ImmA binds to apo MTAP tightly with a K_d of 70 nM and a free binding energy of −9.7 kcal/mol for the three active sites of the trimeric enzyme, showing no binding cooperativity. MT-DADMe-ImmA binds even tighter in the first two sites, with a K_d of 40 nM and a ΔG of −10.1 kcal/mol. The dissociation constant of the third site increased to 110 nM, suggesting modest negative cooperativity for binding at the third site. The K_d of phosphate is 17 μM for all three sites, with a ΔG of −6.51 kcal/mol. Binding of the substrate MTA exhibits a K_d of 8 nM for the first site but 700 nM for the latter two sites, exhibiting significant negative cooperativity. Steady-state kinetic analysis gives a K_m of 1.7 μM for MTA with a significant forward commitment, consistent with a K_d of 700 nM but not 8 nM; thus, the effects of phosphate binding substantially alter the MTA-binding parameters.[7,12] MTAP slowly hydrolyzes MTA in the absence of phosphate with a k_{cat} of 5.1 × 10^{-5} s^{-1}. This slow reaction does not affect the ITC experiments under our selected

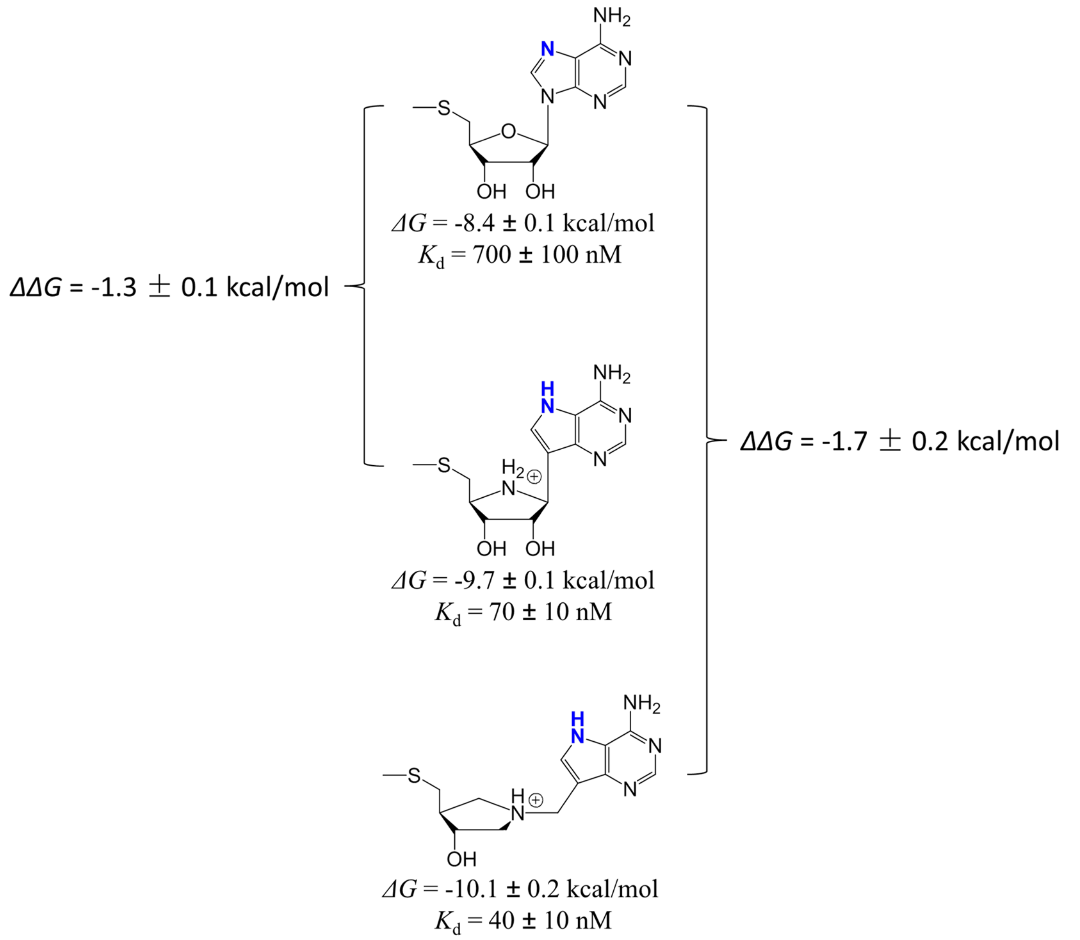

Figure 5. Thermodynamic contributions from the protonated N7 of transition-state analogue inhibitors. The ΔG and K_d values are for the binding of ligands to apo MTAP. The $\Delta\Delta G$ values are calculated by subtracting the ΔG of MTA from those of inhibitors, representing the thermodynamic contributions of protonated N7. The protonation states of N7 are colored in blue.

Table 2. Protonation/Deprotonation Effects on Thermodynamic Parameters of Ligands Binding to Apo MTAP

ligand	ΔH_{Tris} (kcal/mol), [n][a]	$-T\Delta S_{Tris}$ (kcal/mol)	$\Delta H_{Tris} - \Delta H_{Hepes}$ (kcal/mol)	$number_{Proton}$[b]	$\Delta H_{correction}$ (kcal/mol)[c]	$-T\Delta S_{correction}$ (kcal/mol)[c]
MT-ImmA	−12.82 ± 0.05 [3]	3.1 ± 0.1	−3.23 ± 0.09	0.50 ± 0.01	−7.15 ± 0.09	−2.6 ± 0.1
MT-DADMe-ImmA	−11.4 ± 0.2 [2]	1.3 ± 0.3	−1.2 ± 0.8	0.2 ± 0.1	−9.2 ± 0.9	−0.9 ± 0.9
	−10.3 ± 0.4 [1]	0.8 ± 0.4	−7 ± 1	1.1 ± 0.2	2 ± 1	−12 ± 1
phosphate	−2.77 ± 0.04 [3]	−3.74 ± 0.07	5.9 ± 0.3	−0.91 ± 0.05	−13.1 ± 0.4	6.6 ± 0.4

[a] n is the number of sites. [b] Number of protons released from the binding of ligand to MTAP. The ionization enthalpy of Hepes and Tris buffers are 4.876 and 11.341 kcal/mol, respectively.[16] The enthalpy change of $\Delta H_{Tris} - \Delta H_{Hepes}$ is −6.465 kcal/mol for each proton released from the binding complex. [c] $\Delta H_{correction}$ and $-T\Delta S_{correction}$ represent the ΔH and $-T\Delta S$ without any effects from the protonation or deprotonation during the binding.

experimental conditions. However, the hydrolytic reaction reinforces the dissociative catalytic mechanism of MTAP, showing formation of the ribocationic TS with weak participation of the phosphate nucleophile. The MTAP/MTA complexes are capable of reaching the TS without phosphate, albeit with a higher barrier than with phosphate.

Previous studies have shown that the binding of TS analogue inhibitors to the MTAP/phosphate complex is completely driven by entropy, which is interpreted as the result of protein contraction and the exclusion of water from the active site and protein trimeric interfaces.[12] The entropic term ($-T\Delta S$) for MTA binding to the first (tight) site is −10.1 kcal/mol, dominating the ΔG of −11.1 kcal/mol. This thermodynamic pattern is distinct from the binding of other ligands to apo MTAP and to the binding of MTA to the remaining two sites, but it is consistent with the binding of TS analogues to the MTAP/phosphate complex (Table 1). In the first site, MTA forms a ternary complex with water and MTAP and achieves a tight binding affinity, as indicated by the ability of the complex to acquire some part of the TS characteristic. Tightly bound MTA at the first site alters the conformation of the neighboring two subunits to decrease the affinity for the next sites. The K_d values of 700 nM for the latter two sites are similar to the steady-state kinetic parameter for K_m, but the K_m also represents contributions from interaction with phosphate.

Thermodynamic Cycles of Binding TS Analogue Inhibitors. ITC studies on ligands binding to apo enzyme were combined with studies of TS analogues binding to the MTAP/phosphate complex, allowing the construction of thermodynamic cycles for each component of binding in

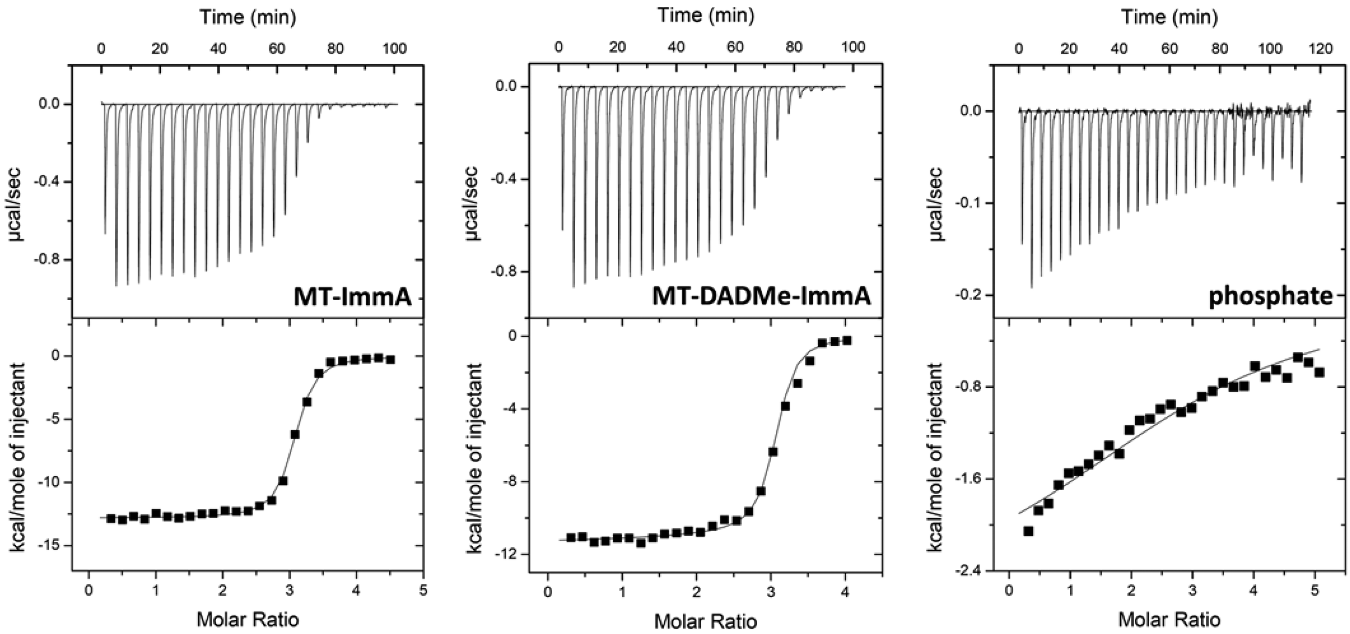

Figure 6. Isothermal titrations of apo MTAP with ligands in Tris Buffer.

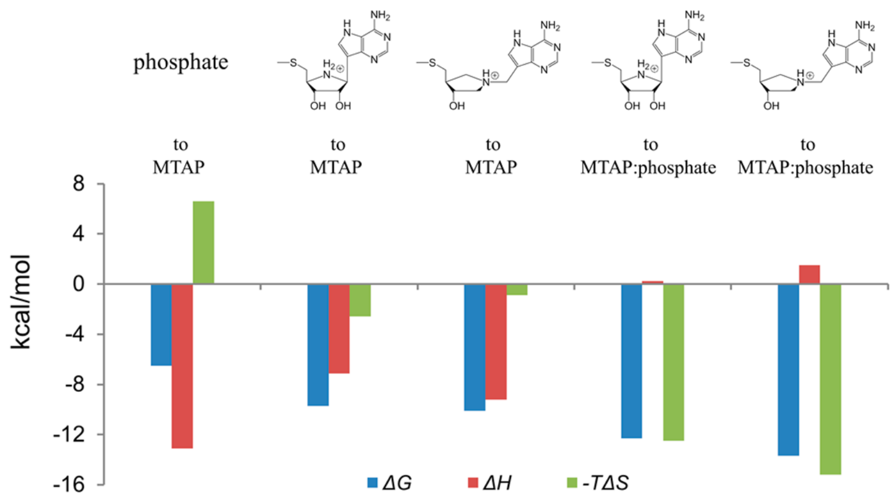

Figure 7. Thermodynamics signatures of ligands binding to MTAP and MTAP/phosphate complex. The thermodynamic parameters of inhibitors binding to MTAP/phosphate complex are from ref 11.

forming the ternary complex with TS analogues (Figures 3 and 4). The ternary TS analogue complex can be obtained through two binding routes provided that random binding is possible. ITC demonstrates that either phosphate or inhibitor can bind first followed by the second ligand. ΔG is a state function and is dependent on only the initial and final states but not the path taken in the cycle. Therefore, $\Delta G_1 + \Delta G_2 = \Delta G_3 + \Delta G_4$ (Figures 3 and 4). At fixed temperature, ΔG is a function of the dissociation constant, defined as $RT\ln K_d$. Thus, the dissociation constants follow the relationship $K_{d1} \times K_{d2} = K_{d3} \times K_{d4}$. The ΔG and K_d values for binding phosphate to the MTAP/inhibitor complex are derived from these equations. The $\Delta\Delta G$ is calculated from $\Delta G_2 - \Delta G_3$, representing the coupling free energy for the interactions between phosphate and the TS analogues. Because the interactions are mainly contributed by the cationic nitrogen-phosphate ion pair, the $\Delta\Delta G$ value provides the thermodynamic contributions from the cationic nitrogen of the TS analogue.

The crystal structure of MTAP in complex with phosphate and MT-ImmA shows interactions between phosphate and MT-ImmA to include two hydrogen bonds to the 2′- and 3′-hydroxyl groups of the inhibitor and an ion pair between phosphate and the cationic nitrogen.[5] The phosphate-specific interactions contribute a $\Delta\Delta G$ value of −2.6 kcal/mol and increase the affinity of MT-ImmA from 70 nM without phosphate to 1 nM in the ternary complex. The crystal structure of MTAP in complex with phosphate and pClPhT-DADMe-ImmA shows a single phosphate/inhibitor interaction (the ion pair between phosphate and the cationic nitrogen).[12] pClPhT-DADMe-ImmA and MT-DADMe-ImmA both belong to the second generation of ImmAs, with the only difference being the remote 5′-methylthio substituent. Therefore, they are expected to exhibit the same contacts with phosphate. The single ion pair in the complex of MTAP/phosphate/MT-DADMe-ImmA is estimated to exhibit a $\Delta\Delta G$ value of −3.6 kcal/mol, which is more favorable than the −2.6 kcal/mol $\Delta\Delta G$ from three interactions formed to MT-ImmA, including

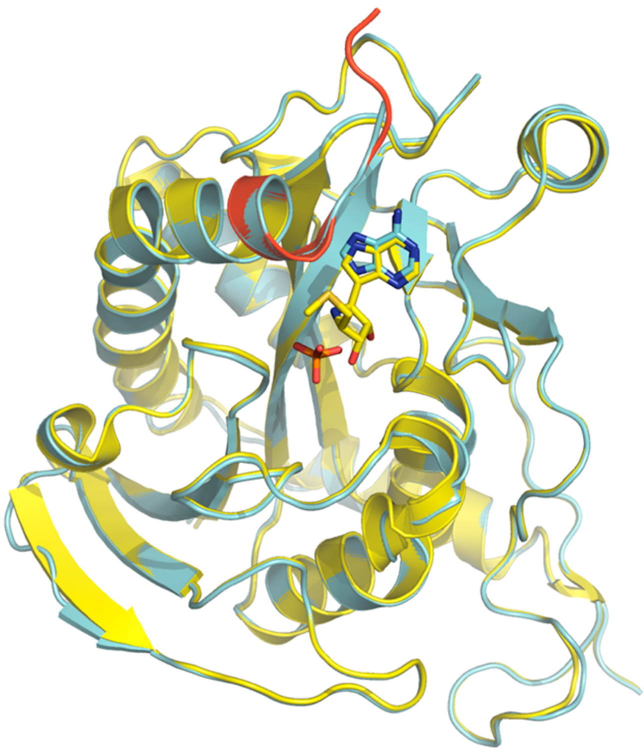

Figure 8. Superimposed structures of MTAP in complex with adenine (PDB ID: 1CB0) and in complex with phosphate and MT-ImmA (PDB ID: 1K27). 1CB0 and 1K27 are colored in cyan and yellow, respectively. The ligands are shown as sticks. The loop composed of residues 227−235 is responsible for the closure of the active site upon transition-state analogues binding to the MTAP/phosphate complex and is colored in red. This loop is flexible in the crystal structure of apo MTAP but fully ordered in the structure of MTAP in complex with phosphate and pClPhT-DADMe-ImmA (a 10 pM second-generation transition-state analogue). Residues 227−229 of the loop are not ordered in 1CBO, whereas in 1K27, only residue 227 is mobile.

an ion pair formed by the same cationic nitrogen and phosphate. This energy difference indicates that the cationic nitrogen of MT-DADMe-ImmA is better positioned to form a thermodynamic-favored ion pair and supports the proposal that MT-DADMe-ImmA more accurately resembles the enzymatic TS. Optimal TS analogues must capture both the geometry and the charges at the TS to achieve the highest binding affinity. In this case, the extra binding free energy decreases the K_d of MT-DADMe-ImmA 440-fold, from 40 nM to 90 pM.

The thermodynamic cycles reveal that the MTAP/inhibitor complexes bind phosphate tighter than the apo enzyme; thus, bound inhibitors provide optimization of the phosphate binding site. Therefore, phosphate and TS analogue free energy of binding is synergistic and is independent of which is bound first. In terms of a physiological interpretation of how TS analogues will interact with MTAP, with a K_d for phosphate of only 17 μM, which is much lower than the mM phosphate concentration of cells, the inhibitor would primarily bind to MTAP/phosphate complexes rather than the apo MTAP.

Thermodynamic Contributions from the 9-Deazaadenine of TS Analogues. The natural substrate MTA is unprotonated at N7, but TS analogue inhibitors are protonated at N7. Crystal structures of MTAP in complex with MTA or MT-ImmA suggest that the interactions between enzyme and these catalytic site ligands are nearly identical except for the hydrogen bond formed between Asp220 and N7. Asp220 is anticipated to be anionic for hydrogen bonding to the N7 of the deazaadenine but neutral for hydrogen bonding to the N7 of adenine. TS analysis suggests an anionic leaving group at the MTAP TS but with H-bond formation to N7 by Asp220; thus, the TS analogue gains a thermodynamic advantage from N7 hydrogen-bond formation with Asp220.[7] The MTAP structure in complex with pClPhT-DADMe-ImmA has the same set of interactions between the 9-deazaadenine group and enzyme as the MT-ImmA structure, and it is not influenced by the relatively large 5′-pClPh group or the 2′-deoxy group,[5,12] predicting the same interactions at the N7 for MT-DADMe-ImmA. Both pClPhT-DADMe-ImmA and MT-DADMe-ImmA are missing the 2′-OH group, which forms a hydrogen bond with the peptide backbone of residue Met196. Therefore, the binding of MT-DADMe-ImmA to MTAP is different from that of MTA in two aspects: an altered pK_a at N7 for optimal hydrogen bonding to Asp220 and one less hydrogen bond with Met196. There are no nearby interactions between the cationic nitrogen of inhibitors or the C4′ oxygen of MTA to the enzyme. Therefore, the cationic nitrogen features of TS

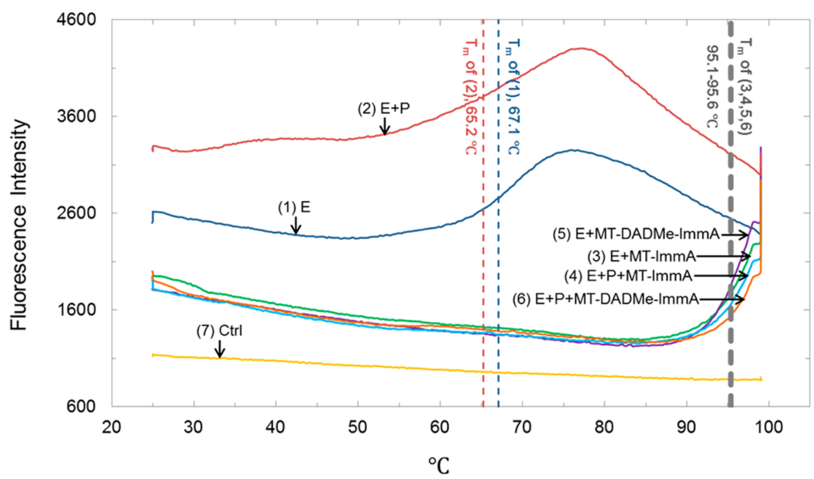

Figure 9. Differential temperature scanning fluorimetry of MTAP. P represents 20 mM phosphate. T_m values (°C) are 67.07 ± 0.08 (1), 65.23 ± 0.08 (2), 95.09 ± 0.07 (3), 95.10 ± 0.08 (4), 95.14 ± 0.06 (5), and 95.61 ± 0.07 (6), respectively. Other conditions are summarized in the Materials and Methods.

analogues are not directly involved in ligand contacts to the apo enzyme. It is, however, possible that the presence of the cationic nitrogen in TS analogues could cause remote electrostatic interactions not detected in crystal structures.

The binding free energy of MTA, MT-ImmA, and MT-DADMe-ImmA to apo MTAP allows the estimation of thermodynamic contributions from the 9-deazaadenine ring, which are reflected in the $\Delta\Delta G$ values calculated by subtracting the binding free energy of MTA from those of inhibitors (Figure 5). MT-ImmA has a $\Delta\Delta G$ value of −1.3 kcal/mol relative to MTA, attributed to the 9-deazaadenine feature of altered pK_a at N7. A $\Delta\Delta G$ value of −1.7 kcal/mol is determined for MT-DADMe-ImmA, suggesting that the thermodynamic advantage from the 9-deazaadenine feature overcomes the disadvantage of losing the 2′-OH hydrogen bond and improves the binding free energy to the enzyme compared to MT-ImmA. First and second generations of TS analogues possess the same 9-deazaadenine leaving group with elevated pK_a at N7, but the second-generation inhibitor, MT-DADMe-ImmA, gains more thermodynamic advantage from the feature, emphasizing the importance of appropriate geometry of the TS analogue.

Protonation/Deprotonation Effects on Thermodynamic Parameters. The binding of ligands to protein may couple to the release or absorption of protons from the complex. In solution, the protons exchange with buffer to cause an ionization enthalpy. The protonation/deprotonation effects can be evaluated by performing the same ITC experiments in two buffers with different ionization enthalpies, a documented technique.[15] In this study, Hepes and Tris buffers were chosen with ionization enthalpies of 4.876 and 11.341 kcal/mol, respectively. Thus, proton release from the MTAP/ligand complex will cause an additional enthalpy change of −6.465 kcal/mol for $\Delta H_{Tris} - \Delta H_{Hepes}$.[16] The differential ΔH values can be used to estimate the number of protons exchanged with buffer and to correct the protonation/deprotonation effects on the ΔH values of ligands ($\Delta H_{correction}$) (Table 2).

The dissociation constants of ligands obtained from ITC experiments in Hepes were used for the fitting of the ITC data from Tris buffer. Binding enthalpies for MT-ImmA, MT-DADMe-ImmA, and phosphate were affected by the buffer selection (Figure 6). Thus, the binding enthalpy for those ligands allows analysis of the protonation/deprotonation effects. The binding of MT-ImmA to apo MTAP releases 0.5 protons into the buffer solution. MT-DADMe-ImmA binding releases 0.2 protons for the binding to the first two sites of trimeric MTAP but 1.1 protons for the binding of the third site, suggesting different catalytic-site ionizations between the first two and the third sites upon binding, consistent with the negative binding cooperativity observed in the isothermal titrations (Figures 2 and 6). At pH 7.4, 80% of the phosphates are dibasic. ITC data indicates that phosphate binds to apo MTAP with an absorption of 0.91 ± 0.05 protons from the buffer, implicating either monobasic bound phosphate or an enzyme group that becomes protonated upon dibasic-phosphate binding.

The corrected ΔH ($\Delta H_{correction}$) and $-T\Delta S$ ($-T\Delta S_{correction}$) values are the binding enthalpy and entropy without protonation or deprotonation effects, representing the intrinsic thermodynamic signatures of ligand binding (Table 2 and Figure 7). Previous studies revealed that binding of TS analogues to MTAP/phosphate is completely driven by entropy with an enthalpic penalty. This observation was explained by the closing of enzyme active site and the overall compacting of the trimeric structure, causing the exclusion of water from the active site and subunit interfaces and thereby dominating the entropy term. In contrast, the binding of individual phosphate and TS analogues to apo MTAP shows distinct thermodynamic signatures, with enthalpy as the major contributor. MT-ImmA and MT-DADMe-ImmA bind to apo MTAP with a $\Delta H_{correction}$ of −7.15 and −9.2 kcal/mol, respectively, accounting for 74 and 91% of the total binding free energy for each inhibitor. The $\Delta H_{correction}$ of phosphate is −13.1 kcal/mol, and it pays a strong entropic penalty of 6.6 kcal/mol. Phosphate and TS analogues all bind enthalpically, reflecting the formation of favorable hydrogen or ionic bonds but an enzyme active site that remains open. The large entropic penalty on phosphate binding suggests a loss of dynamic structure surrounding the phosphate-binding site upon binding. The results indicate that it is the interaction between phosphate and TS analogue that closes the active site, expels water, and converts binding enthalpy to entropy. Crystal structures of apo MTAP and MTAP in complex with TS analogues and phosphate have revealed that the binding of phosphate caused no significant conformational changes to the MTAP structures, but the binding of TS analogues causes the closure of the active site by the motion of a loop (residue 227−235) that is flexible in the apo enzyme but closed in the complexes.[12] The overlay of the structures of MTAP in complex with adenine (PDB ID: 1CB0) and in complex with phosphate and MT-ImmA (PDB ID: 1K27) show that the inhibitor MT-ImmA is pulled toward the phosphate with a more ordered loop of residues 227−235 (Figure 8). Phosphate is the anchor for the TS analogues, and their ion-pair formation provides the driving force to cause the active site to close. Although the protein is proposed to become more organized (less dynamic), normally an entropic penalty, the altered water access to the protein is proposed to dominate for a net entropic driving force for the closed complex.

Testing MTAP Stability in the Ternary Complexes. Thermodynamic data for MTAP revealed that the overall binding of inhibitors was driven by favorable entropy, supporting a more disordered state. However, we propose that the ternary complexes are more thermodynamically stable than apo MTAP or binary complexes on the basis of the unique enthalpy−entropy converting mechanism of this enzyme at its TS. Our hypothesis was tested using differential temperature scanning fluorimetry. Apo MTAP gave a T_m of 67.1 °C, and the binary complex with phosphate decreased stability slightly to 65.7 °C (Figure 9). Binding of MT-ImmA or MT-DADMe-ImmA in binary or ternary complexes showed a remarkable ability to stabilize the protein, with T_m values of 95.1−95.6 °C for all complexes with TS analogues. Thus, the entropic contributions found in the ternary TS complexes are not on the path to dynamic unfolding, but they induce extraordinary thermal stability. This finding is consistent with structural and heat capacity changes that altered hydrophobic interactions and resulted in the release of water upon binding of TS analogues to MTAP.[11]

■ CONCLUSIONS

MTAP catalyzes the phosphorolysis of MTA and requires the simultaneous binding of MTA and phosphate to generate the TS. The enzyme binds phosphate and TS analogues independently to form stable, enthalpy-driven binary interactions. Formation of the ternary complex with enzyme, TS analogue, and phosphate causes a large, favorable entropic change, reflecting a conformational change in the protein that excludes water from the catalytic site and subunit interfaces of the protein. The driving force for the formation of the entropically favorable ternary complex is an enzyme-bound ion pair between the anionic phosphate and cationic TS analogues. Binary MTAP/TS analogue or ternary MTAP/TS analogue/phosphate complexes demonstrate remarkable thermal stability with a T_m near 95 °C, a ΔT_m of 28 °C compared to apo MTAP.

The substrate MTA shows a binding pattern distinct from the TS analogues. It binds tightly to the first catalytic site, driven by a large and favorable entropy, and binds less tightly to the second and third sites, driven by enthalpy, similar to the binary complexes with phosphate or TS analogues. MTA binding is reminiscent of adenine binding to MTAP/phosphate by showing negative cooperativity and being entropy-driven, suggesting that adenine interactions contribute to the first-site MTA interaction and alter the binding thermodynamics at the remaining two sites.[11]

TS analogue binding is favored by the elevated pK_a of N7 in 9-deazaadenine, and the cationic nitrogen mimic of the ribocation at the TS. Thus, MT-ImmA binds 1700 times and MT-DADMe-ImmA binds 18 900 times tighter than the K_m for MTA.

ITC studies provided the thermodynamic parameters for phosphate, MTA, and TS analogue inhibitors to MTAP. The use of two buffer systems provided estimates of proton release or uptake for the interactions of TS analogues and phosphate.

Thermodynamic characterization of MTAP reveals a unique mechanism of enthalpically favorable binding of phosphate and nucleoside components driving a conformational reorganization with favorable entropic characteristics to deliver the bound reactants toward the TS. This reorganization is revealed by quantitating the conversion of binding enthalpy to entropy in tight complexes with TS analogues.

AUTHOR INFORMATION

Corresponding Author

*Tel.: +1 718 430 2813. Fax: +1 718 430 8565. E-mail: vern.schramm@einstein.yu.edu.

Funding

This work was supported by NIH research grants GM41916 and CA135405.

Notes

The authors declare no competing financial interest.

ABBREVIATIONS USED

MTA, 5′-methylthioadenosine; SAM, S-adenosyl-L-methionine; MTAP, MTA phosphorylase; PNP, purine nucleoside phosphorylase; MTR-1-P, 5-methylthioribose-α-D-1-phosphate; ImmA, Immucillin-A; DADMe, 4′-deaza-1′-aza-2′-deoxy-1′-(9-methylene); TS, transition state

REFERENCES

(1) Williams-Ashman, H. G., Seidenfeld, J., and Galletti, P. (1982) Trends in the biochemical pharmacology of 5′-deoxy-5′-methylthioadenosine. *Biochem. Pharmacol. 31*, 277−288.

(2) Cacciapuoti, G., Oliva, A., and Zappia, V. (1978) Studies on phosphate-activated 5′-methylthioadenosine nucleosidase from human placenta. *Int. J. Biochem. 9*, 35−41.

(3) Kamatani, N., and Carson, D. A. (1981) Dependence of adenine production upon polyamine synthesis in cultured human lymphoblasts. *Biochim. Biophys. Acta, Gen. Subj. 675*, 344−350.

(4) Basu, I., Locker, J., Cassera, M. B., Belbin, T. J., Merino, E. F., Dong, X., Hemeon, I., Evans, G. B., Guha, C., and Schramm, V. L. (2011) Growth and metastases of human lung cancer are inhibited in mouse xenografts by a transition state analogue of 5′-methylthioadenosine phosphorylase. *J. Biol. Chem. 286*, 4902−4911.

(5) Basu, I., Cordovano, G., Das, I., Belbin, T. J., Guha, C., and Schramm, V. L. (2007) A transition state analogue of 5′-methylthioadenosine phosphorylase induces apoptosis in head and neck cancers. *J. Biol. Chem. 282*, 21477−21486.

(6) Camacho-Vanegas, O., Camacho, S. C., Till, J., Miranda-Lorenzo, I., Terzo, E., Ramirez, M. C., Schramm, V., Cordovano, G., Watts, G., Mehta, S., Kimonis, V., Hoch, B., Philibert, K. D., Raabe, C. A., Bishop, D. F., Glucksman, M. J., and Martignetti, J. A. (2012) Primate genome gain and loss: a bone dysplasia, muscular dystrophy, and bone cancer syndrome resulting from mutated retroviral-derived MTAP transcripts. *Am. J. Hum. Genet. 90*, 614−627.

(7) Singh, V., and Schramm, V. L. (2006) Transition-state structure of human 5′-methylthioadenosine phosphorylase. *J. Am. Chem. Soc. 128*, 14691−14696.

(8) Singh, V., Shi, W., Evans, G. B., Tyler, P. C., Furneaux, R. H., Almo, S. C., and Schramm, V. L. (2004) Picomolar transition state analogue inhibitors of human 5′-methylthioadenosine phosphorylase and X-ray structure with MT-Immucillin-A. *Biochemistry 43*, 9−18.

(9) Evans, G. B., Furneaux, R. H., Schramm, V. L., Singh, V., and Tyler, P. C. (2004) Targeting the polyamine pathway with transition-state analogue inhibitors of 5′-methylthioadenosine phosphorylase. *J. Med. Chem. 47*, 3275−3281.

(10) Evans, G. B., Furneaux, R. H., Lenz, D. H., Painter, G. F., Schramm, V. L., Singh, V., and Tyler, P. C. (2005) Second generation transition state analogue inhibitors of human 5′-methylthioadenosine phosphorylase. *J. Med. Chem. 48*, 4679−4689.

(11) Guan, R., Ho, M. C., Brenowitz, M., Tyler, P. C., Evans, G. B., Almo, S. C., and Schramm, V. L. (2011) Entropy-driven binding of picomolar transition state analogue inhibitors to human 5′-methylthioadenosine phosphorylase. *Biochemistry 50*, 10408−10417.

(12) Appleby, T. C., Erion, M. D., and Ealick, S. E. (1999) The structure of human 5′-deoxy-5′-methylthioadenosine phosphorylase at 1.7 angstrom resolution provides insights into substrate binding and catalysis. *Structure 7*, 629−641.

(13) Edwards, A. A., Mason, J. M., Clinch, K., Tyler, P. C., Evans, G. B., and Schramm, V. L. (2009) Altered enthalpy−entropy compensation in picomolar transition state analogues of human purine nucleoside phosphorylase. *Biochemistry 48*, 5226−5238.

(14) Miles, R. W., Tyler, P. C., Furneaux, R. H., Bagdassarian, C. K., and Schramm, V. L. (1998) One-third-the-sites transition-state inhibitors for purine nucleoside phosphorylase. *Biochemistry 37*, 8615−3621.

(15) Gomez, J., and Freire, E. (1995) Thermodynamic mapping of the inhibitor site of the aspartic protease endothiapepsin. *J. Mol. Biol. 252*, 337−350.

(16) Niesen, F. H., Berglund, H., and Vedadi, M. (2007) The use of differential scanning fluorimetry to detect ligand interactions that promote protein stability. *Nat. Protoc. 2*, 2212−2221.